Interaction of Copper(II) (3+2)N-Chelating Complexes with DNA and BSA: Hydrolytic DNA Cleavage and ROS-Mediated Apoptosis

Mariappan Murali,[a]* Anbarasu Kanchana Mala,[b] Somasundaram Sangeetha[a],[c] Balasubramaniam Selvakumaran,[a] Pitchan Arul Prakash,[d] Selvaraj Shanmugavadivel,[a] Tamilarasan Ajay Kamal,[e] Mohamed Sultan Mohamed Jaabir[d]

[a]*Coordination and Bioinorganic Chemistry Research Laboratory, Department of Chemistry, National College (Autonomous), Tiruchirappalli 620 001 Tamil Nadu, India*

[b]*Department of Pharmacology, Saveetha Institute of Medical and Technical Sciences, Chennai 600 124 Tamil Nadu, India.*

[c]*Department of Chemistry, Tamilavel Umamaheswaranar Karanthai Arts College, Thanjavur 613 002, Tamil Nadu, India dDepartment of Biotechnology and Microbiology, National College (Autonomous),Tiruchirappalli 620 001, Tamil Nadu, India*

[e]*Center for Advanced Energy Materials, SRM TRP Engineering College, Tiruchirappalli - 621 105, Tamil Nadu, India; Centre for Research, Trichy SRM Medical College Hospital and Research Center, Tiruchirappalli, 621105,.*

*Corresponding author: Mariappan Murali - e-mail: murali@nct.ac.in and ma66mu@gmail.com

Phone: +91-431-2482995 / Fax: +91-431-2481997

Table S1 Selected crystal data and structure refinement parameters for **2**

Formula	$C_{26}H_{23}Cl_2N_5O_8Cu$
Formula weight	667.93
Temperature (K)	296(2)
Wavelength (Å)	0.71073
Crystal system	Monoclinic
Space group	$P2_1/c$
a (Å)	16.2038(10)
b (Å)	11.7856(8)
c (Å)	15.4244(10)
α (°)	90
β (°)	108.735(2)
γ (°)	90
V (Å)^3, Z	2789.5(3), 4
D_{calc} (mg m^{-3})	1.590
μ (mm^{-1})	1.033
F(000)	1364
Crystal size (mm^3)	0.350 × 0.320 × 0.210
θ (°)	2.179 to 24.998
Index ranges	-19 ≤ h ≤ 19
	-13 ≤ k ≤ 14
	-18 ≤ l ≤ 16
Reflections collected	19061
Independent reflections	4879
Reflections observed [I > 2σ(I)]	4069
R_{int}	0.0300
GOOF	1.048
R_1 [I > 2σ(I)]	0.0397
wR_2 [I > 2σ(I)]	0.0994
R_1, wR_2 all data	0.0507/0.1087

Table S2 Ligand-based absorption spectral properties[a] and fluorescence spectral properties[b] of copper(II) complexes (**1** and **2**) bound to CT DNA

Complex	λ_{max} (nm)	Ligand-based					
		R	Change in absorbance	Δε (%)	Red-shift (nm)	K_b (× 10^5 M^{-1})	K_{app}[b](× 10^6 M^{-1})
$[Cu(L1)(phen)]^{2+}$ **1**	268	25	Hypochromism	60	3	1.355± 0.001	5.2
$[Cu(L2)(phen)]^{2+}$ **2**	268	25	Hypochromism	32	2	1.056± 0.001	5.0

[a]Measurements were made at R = 25, where R = [DNA]/[complex]; the concentration of solutions of Cu(II) complexes = 10 × 10^{-6} M (**1** and **2**). [b]Apparent DNA binding constant from the ethidium bromide displacement assay using increasing concentrations (0-10 μM) of **1** and **2**.

Table S3 Quenching, association, binding and thermodynamic parameters of the interaction of **1** and **2** with BSA at different temperatures

Parameters	300 K	R	310 K	R
[Cu(L1)(phen)](ClO$_4$)$_2$ 1				
K_{SV} (10^5 M^{-1}) ± SD	4.306 ± 0.004	0.9991	5.427 ± 0.006	0.9985
k_q (10^{13} M^{-1} s^{-1})	4.306		5.427	
K_a (10^5 M^{-1}) ± SD	1.501 ± 0.016	0.9967	2.2643 ± 0.010	0.9951
K_b (10^6 M^{-1}) ± SD	1.102 ± 0.037	0.9959	1.341 ± 0.012	0.9991
n ± SD	1.101 ± 0.006		1.046 ± 0.004	
ΔH° (kJ mol^{-1})	70.426			
ΔS° (J mol^{-1} K^{-1})	105.293		106.138	
ΔG° (kJ mol^{-1})	-31.954		-32.619	
[Cu(L2)(phen)](ClO$_4$)$_2$ 2				
K_{SV} (10^5 M^{-1}) ± SD	4.075 ± 0.004	0.9986	5.617 ± 0.006	0.9989
k_q (10^{13} M^{-1} s^{-1})	4.075		5.617	
K_a (10^5 M^{-1}) ± SD	3.229 ± 0.006	0.9969	3.8804 ± 0.004	0.9975
K_b (10^6 M^{-1}) ± SD	2.188 ± 0.012	0.9934	2.623 ± 0.015	0.9984
n ± SD	1.163 ± 0.002		1.142 ± 0.006	
ΔH° (kJ mol^{-1})	73.624			
ΔS° (J mol^{-1} K^{-1})	108.326		109.452	
ΔG° (kJ mol^{-1})	-32.613		-34.922	

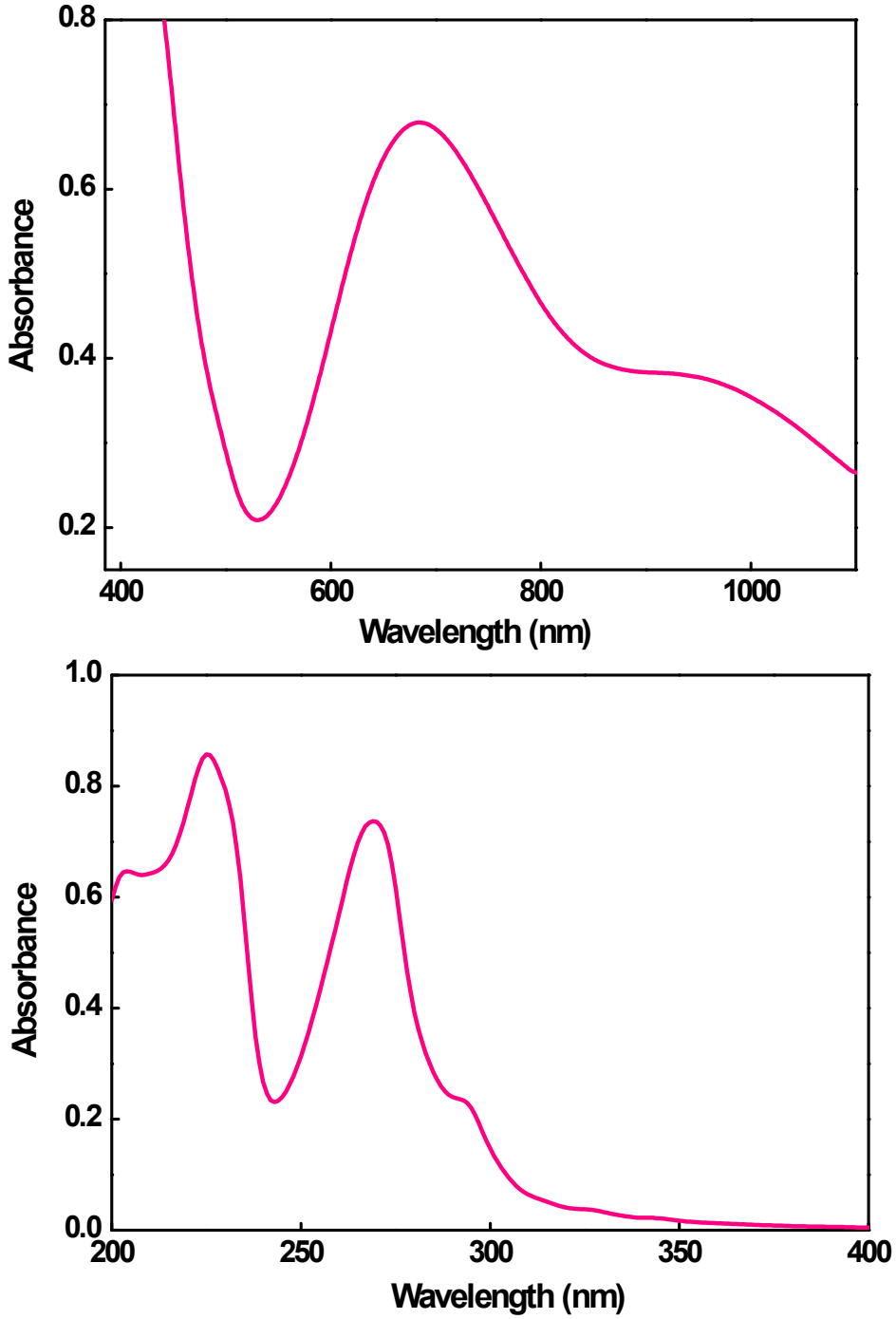

Fig. S1 Electronic spectra of $[Cu(L1)(phen)](ClO_4)_2$ **1** in DMF

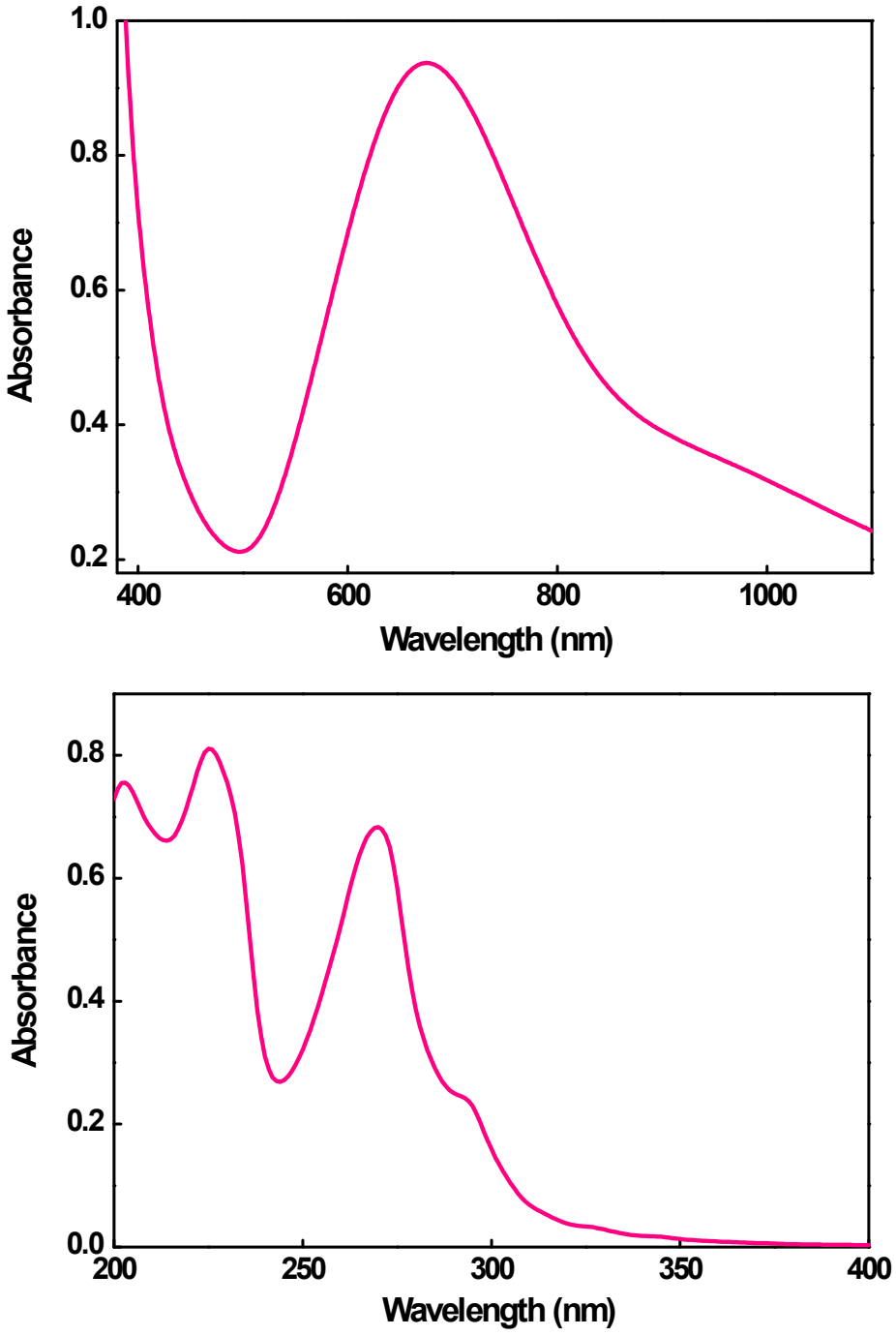

Fig. S2 Electronic spectra of $[Cu(L2)(phen)](ClO_4)_2$ **2** in DMF

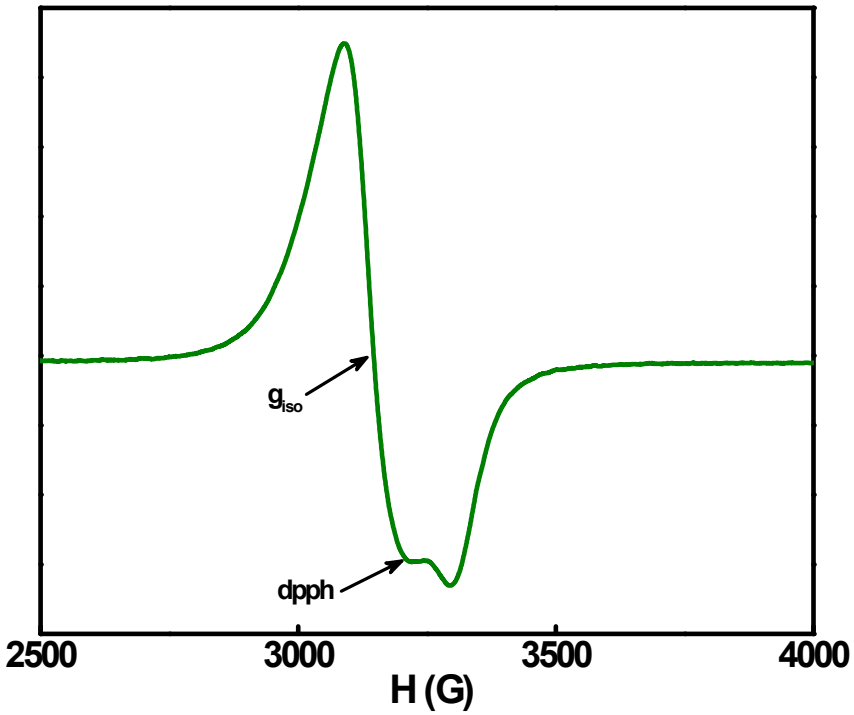

Fig. S3 Polycrystalline EPR spectrum of $[Cu(L1)(phen)](ClO_4)_2$ **1** at RT.

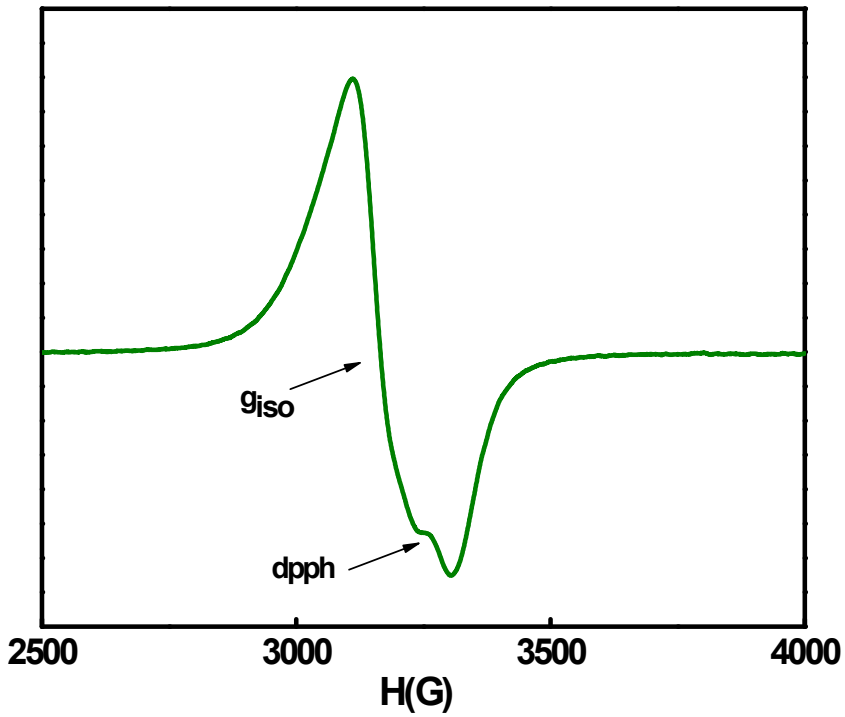

Fig. S4 Polycrystalline EPR spectrum of $[Cu(L2)(phen)](ClO_4)_2$ **2** at RT.

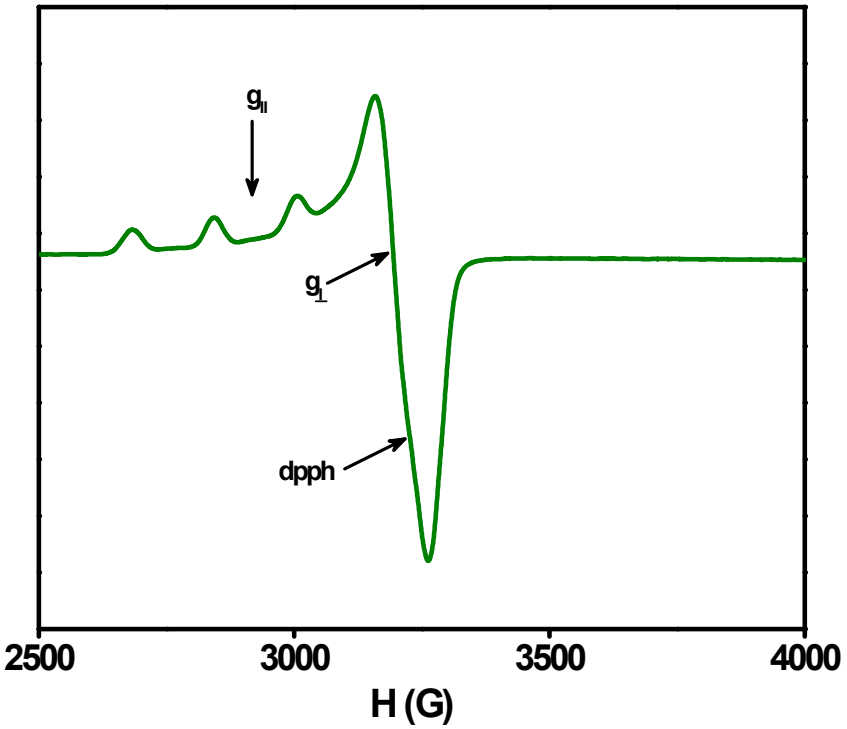

Fig. S5 EPR spectrum of [Cu(L1)(phen)]$(ClO_4)_2$ **1** in DMF at 77 K.

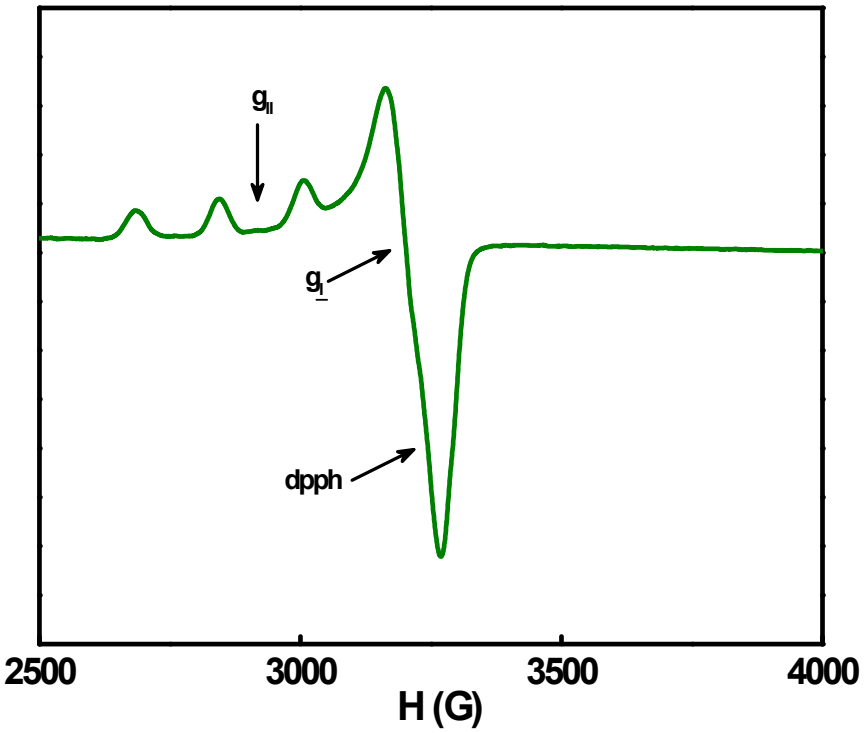

Fig. S6 EPR spectrum of [Cu(L2)(phen)]$(ClO_4)_2$ **2** in DMF at 77 K.

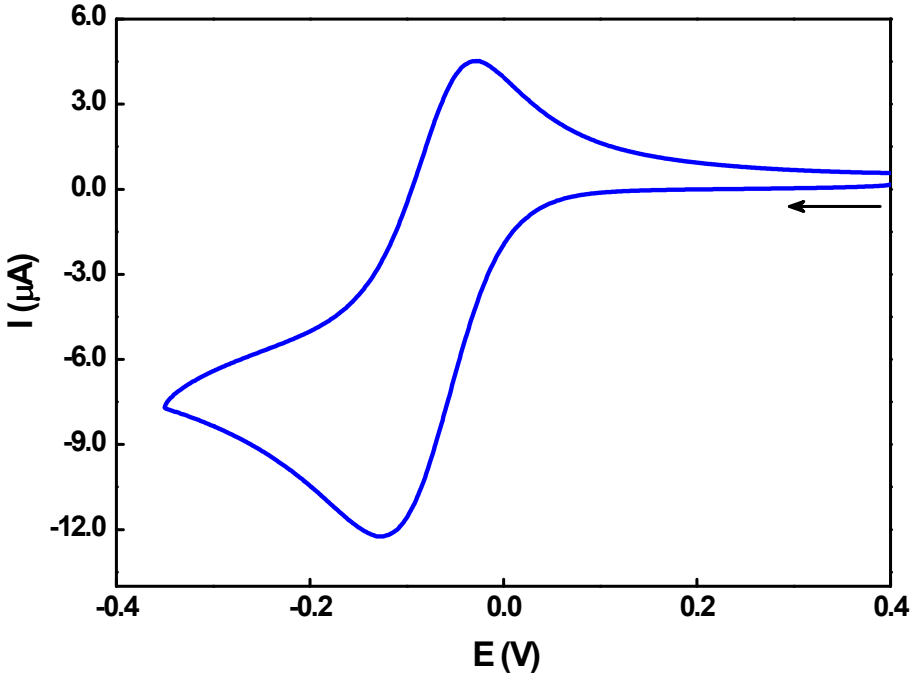

Fig. S7 Cyclic voltammogram of $[Cu(L1)(phen)](ClO_4)_2$ **1** at 50 mV s^{-1} scan rate in DMF

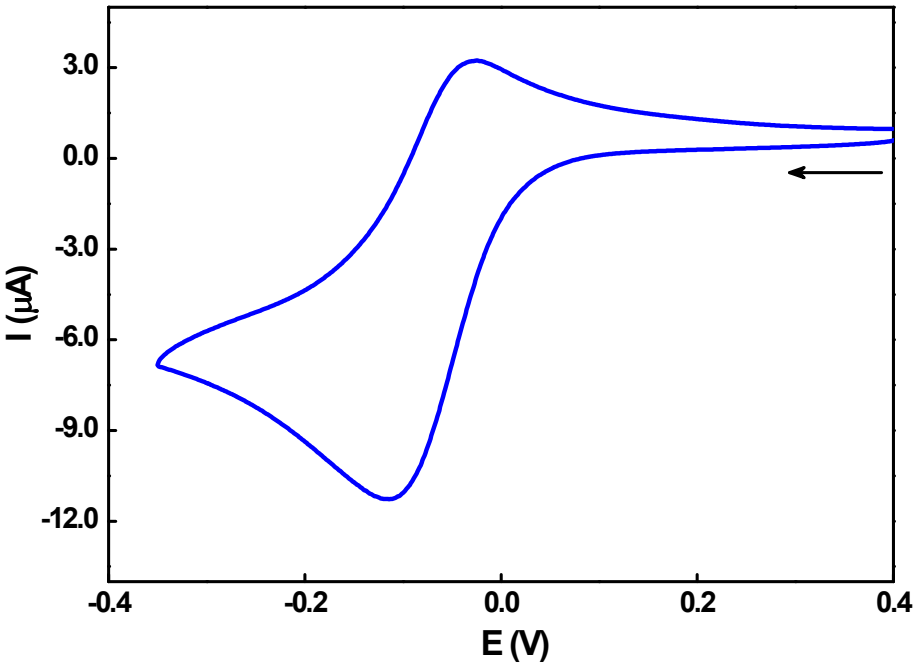

Fig. S8 Cyclic voltammogram of $[Cu(L2)(phen)](ClO_4)_2$ **2** at 50 mV s^{-1} scan rate in DMF

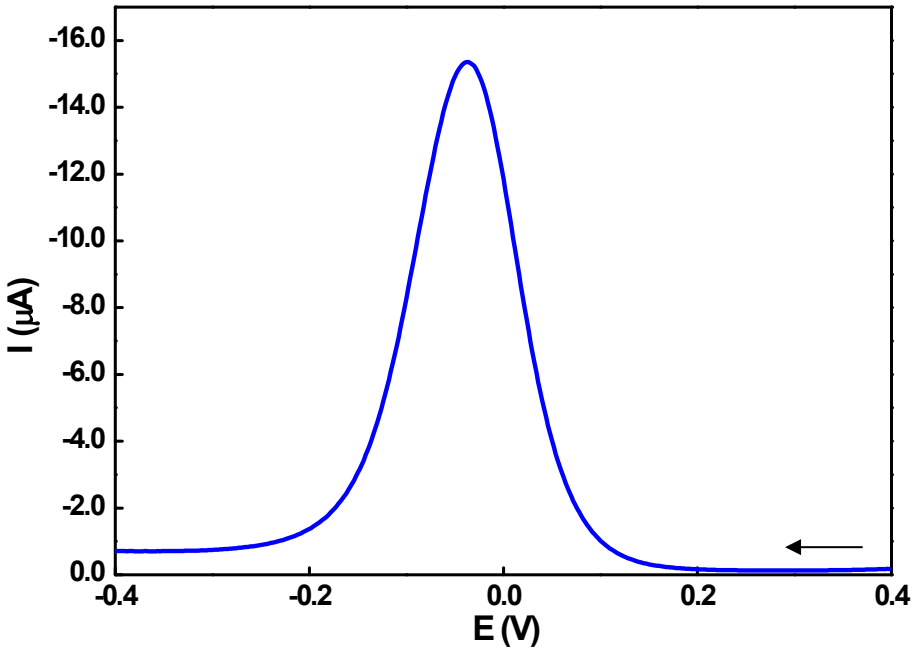

Fig. S9 Differntial pulse voltammogram of $[Cu(L1)(phen)](ClO_4)_2$ **1** at 2 mV s^{-1} scan rate in DMF

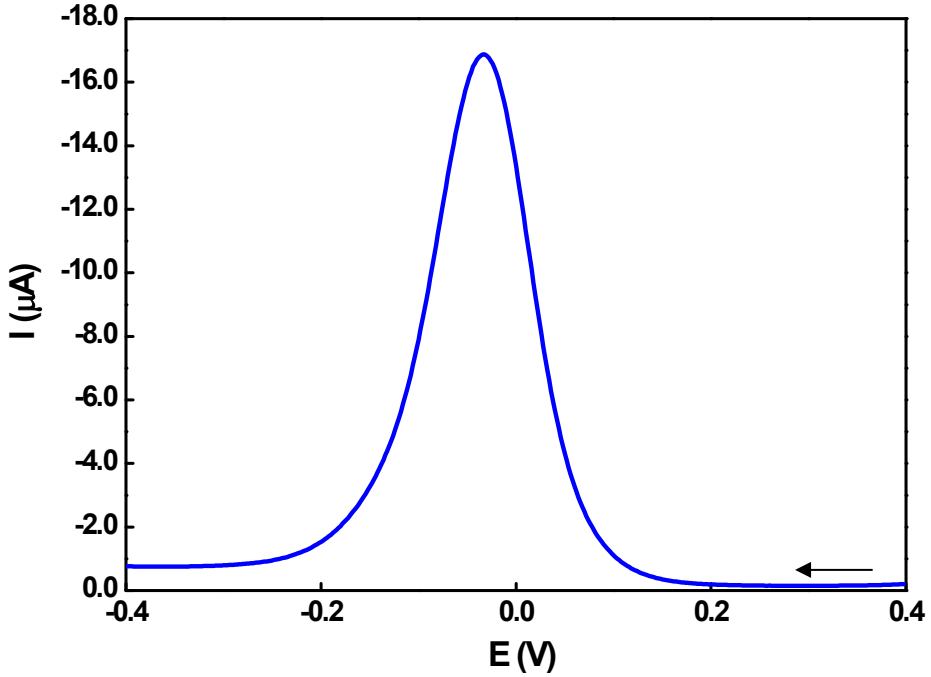

Fig. S10 Differntial pulse voltammogram of $[Cu(L2)(phen)](ClO_4)_2$ **2** at 2 mV s^{-1} scan rate in DMF.

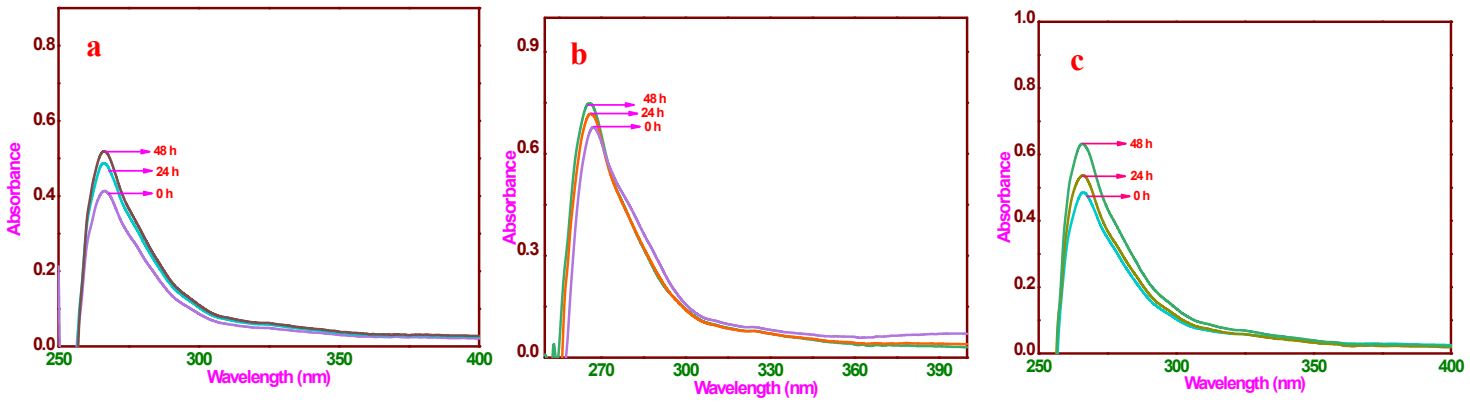

Fig. S11 Electronic spectrum of **1** in (a) DMSO (b) DMF/5 mM Tris-HCl/50 mM NaCl buffer (pH 7.1) (c) DMEM.

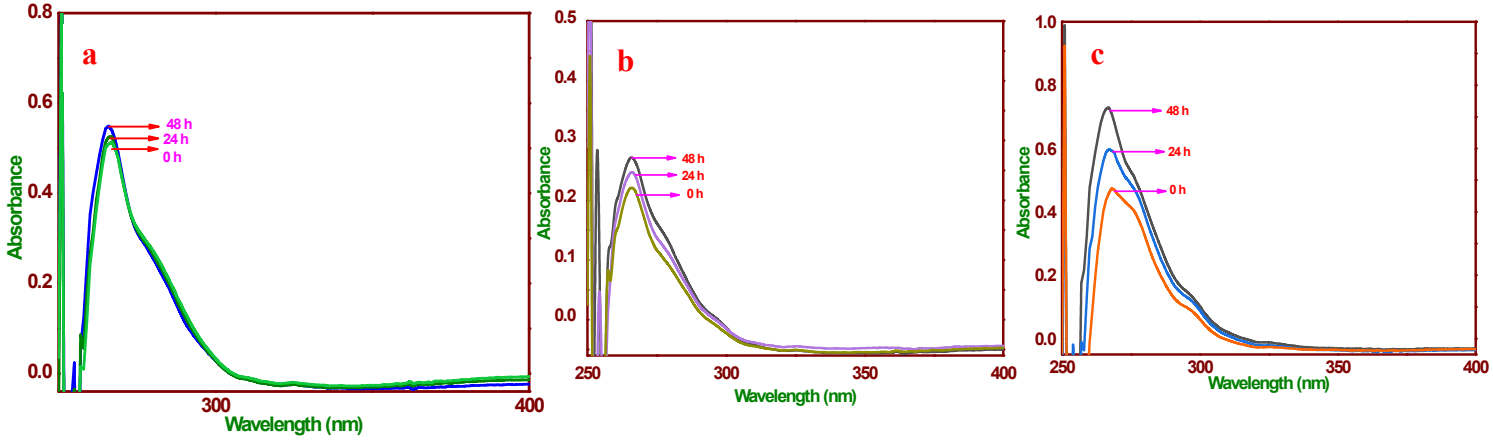

Fig. S12 Electronic spectrum of **2** in (a) DMSO (b) DMF/5 mM Tris-HCl/50 mM NaCl buffer (pH 7.1) (c) DMEM.

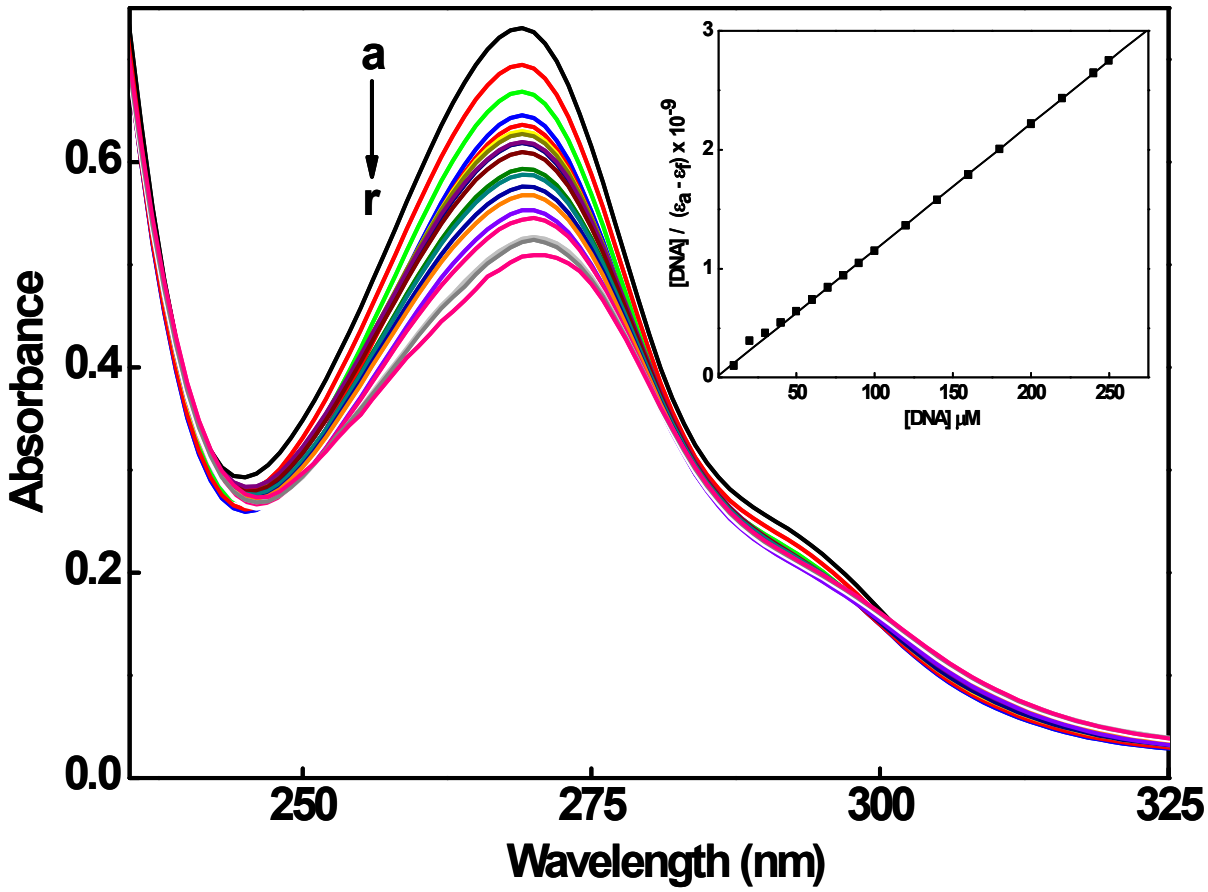

Fig. S13 Absorption spectra of **2** (10×10^{-6} M) in 2% DMF/5 mM Tris-HCl/50 mM NaCl buffer at pH 7.1 in the absence (R = 0) and presence (R = 25) of increasing amounts of CT DNA. Inset: Plot of [DNA] vs [DNA]/(ε_a - ε_f) at R = 25 of **2**.

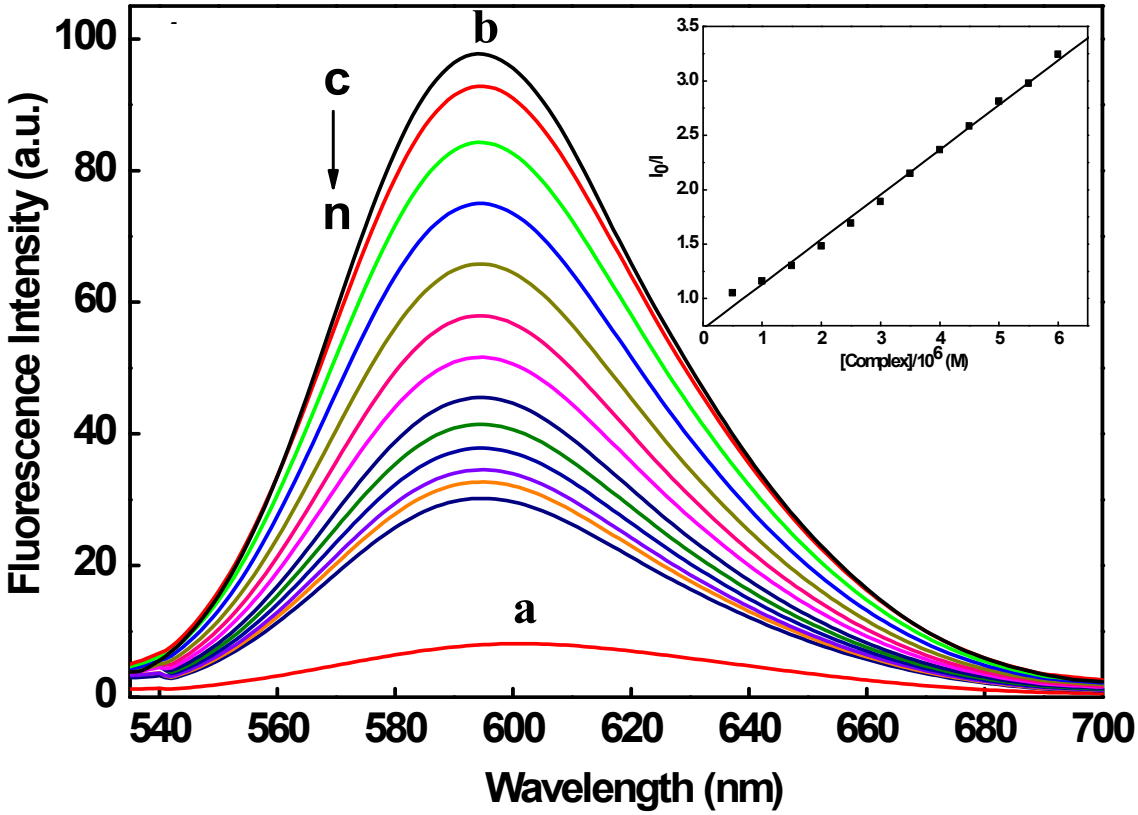

Fig. S14 Fluorescence quenching curves of ethidium bromide bound to DNA in 2% DMF/5 mM Tris-HCl/50 mM NaCl buffer at pH 7.1: (a) EthBr (1.25 μM); (b) EthBr + DNA (125 μM); (c-m) EthBr + DNA + **1** (0-10 μM). Inset: Plot of I_0/I versus [complex].

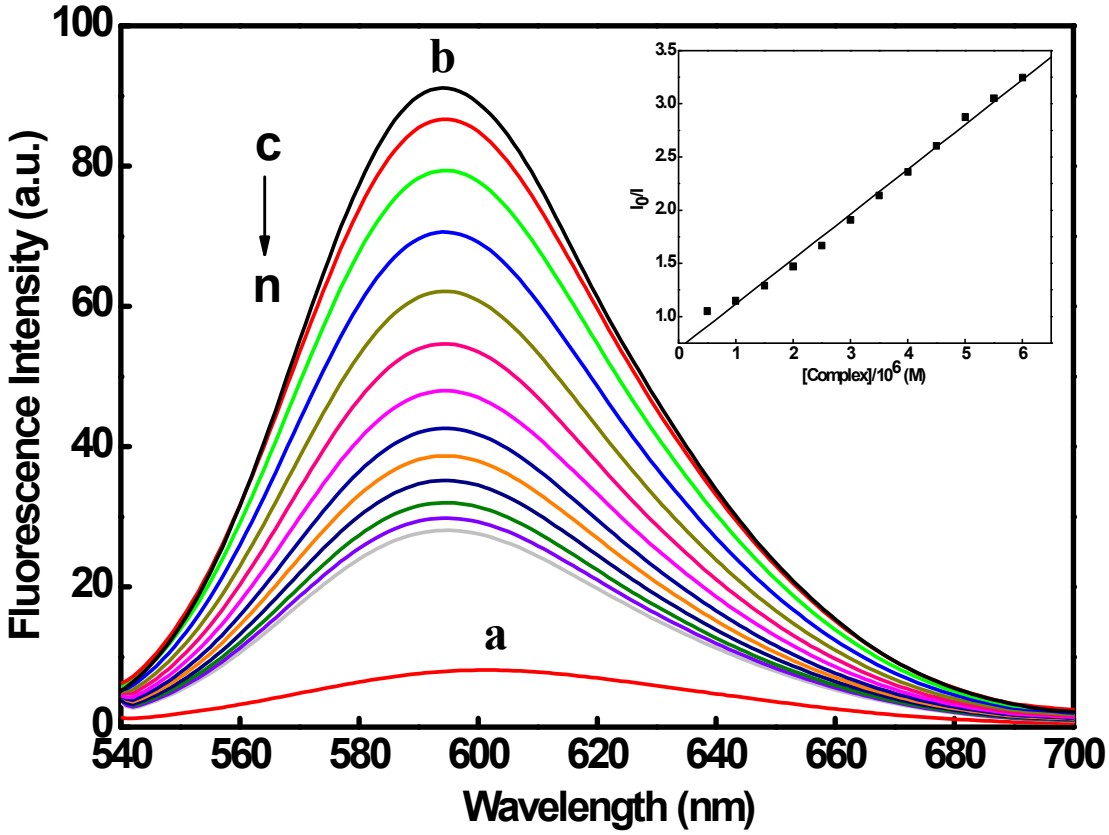

Fig. S15 Fluorescence quenching curves of ethidium bromide bound to DNA in 2% DMF/5 mM Tris-HCl/50 mM NaCl buffer at pH 7.1: (a) EthBr (1.25 μM); (b) EthBr + DNA (125 μM); (c-m) EthBr + DNA + **2** (0-10 μM). Inset: Plot of I_0/I versus [complex].

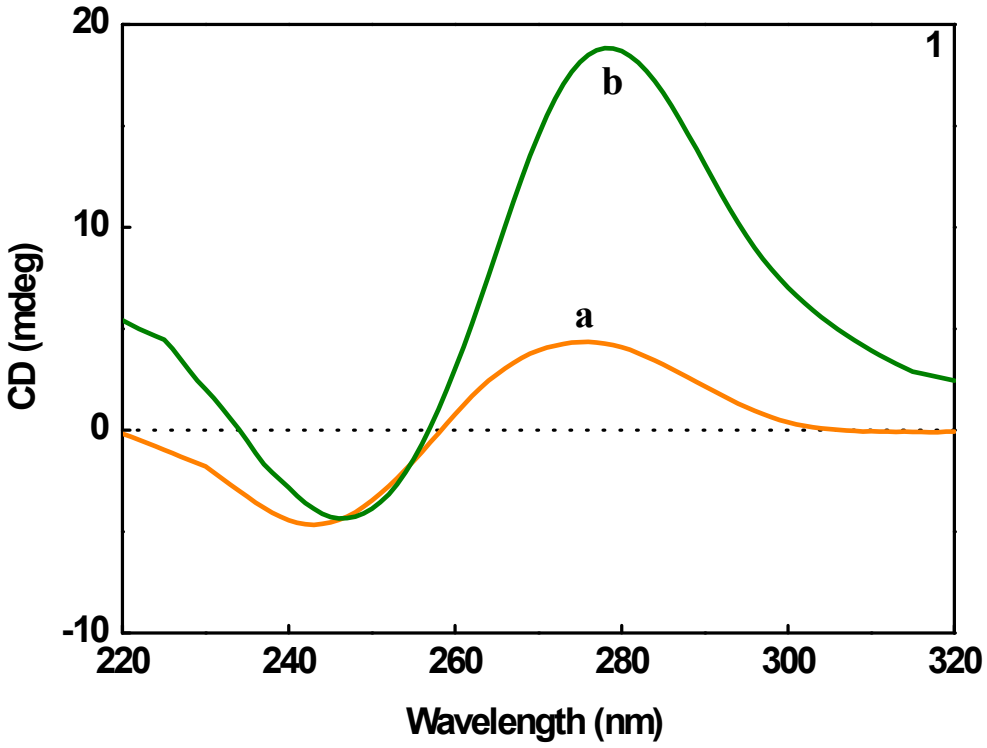

Fig. S16 Circular dichroism spectra of CT DNA in 2% DMF/5 mM Tris-HCl/50 mM NaCl buffer at pH 7.1 and 25 °C in the absence (a) and presence (b) of **1** at 1/R value of 3.

.

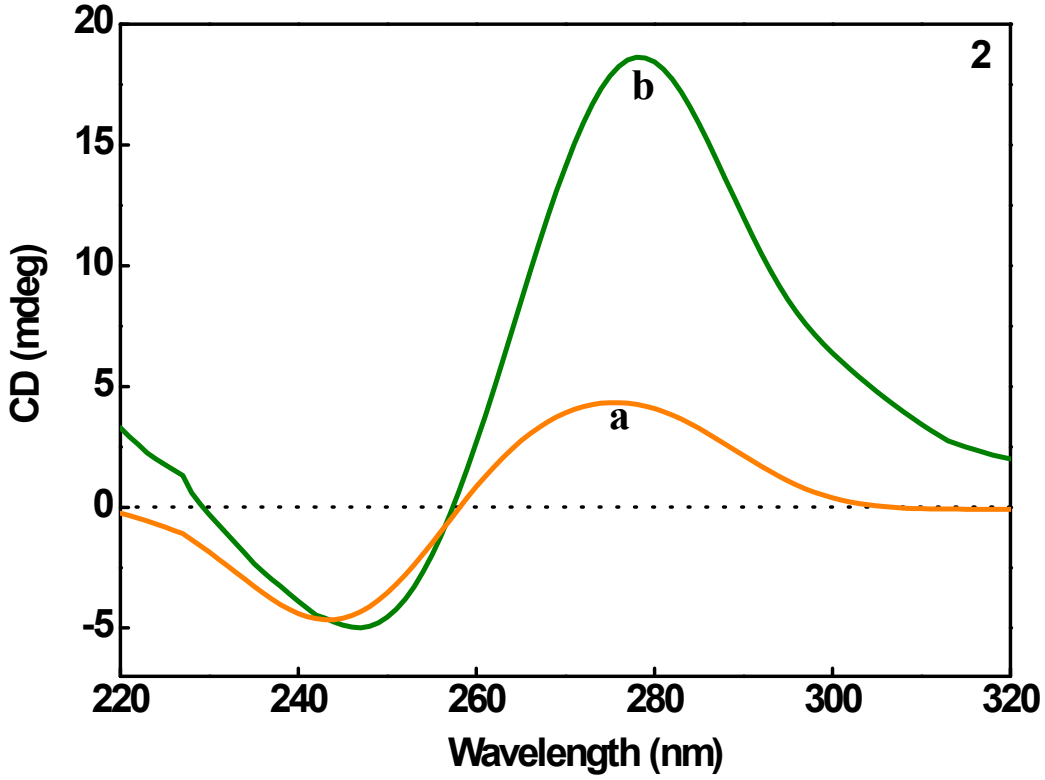

Fig. S17 Circular dichroism spectra of CT DNA in 2% DMF/5 mM Tris-HCl/50 mM NaCl buffer at pH 7.1 and 25 °C in the absence (a) and presence (b) of **2** at 1/R value of 3.

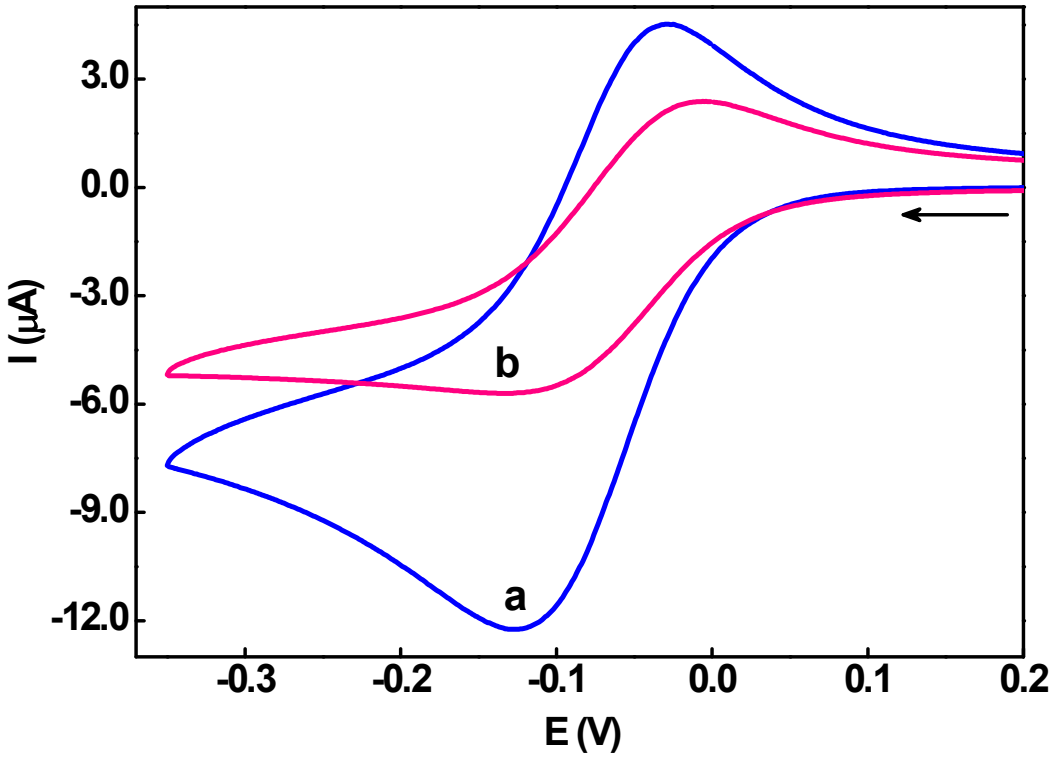

Fig. S18 Cyclic voltammograms of **1** (0.5 mM) in the absence (a) and presence (b) of CT DNA (R = 5) at 25.0±0.2 °C at 50 mV s^{-1} scan rate in 2% DMF/5 mM Tris-HCl/50 mM NaCl buffer at pH 7.1.

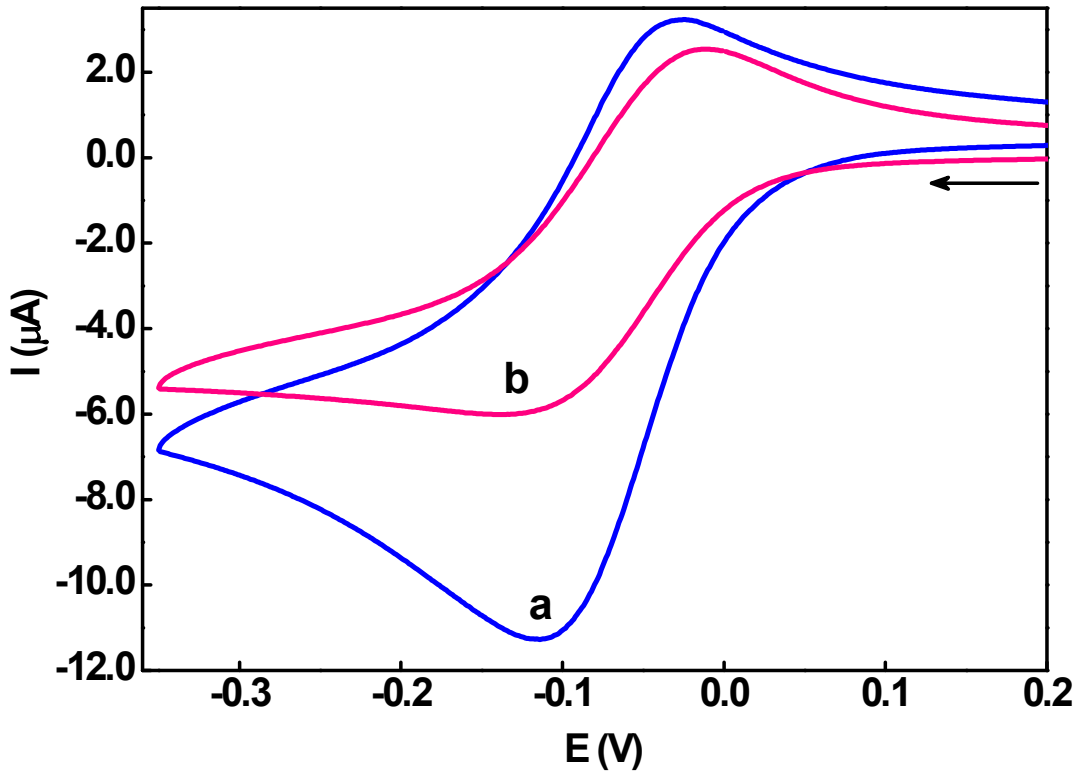

Fig. S19 Cyclic voltammograms of **2** (0.5 mM) in the absence (a) and presence (b) of CT DNA (R = 5) at 25.0±0.2 °C at 50 mV s^{-1} scan rate in 2% DMF/5 mM Tris-HCl/50 mM NaCl buffer at pH 7.1.

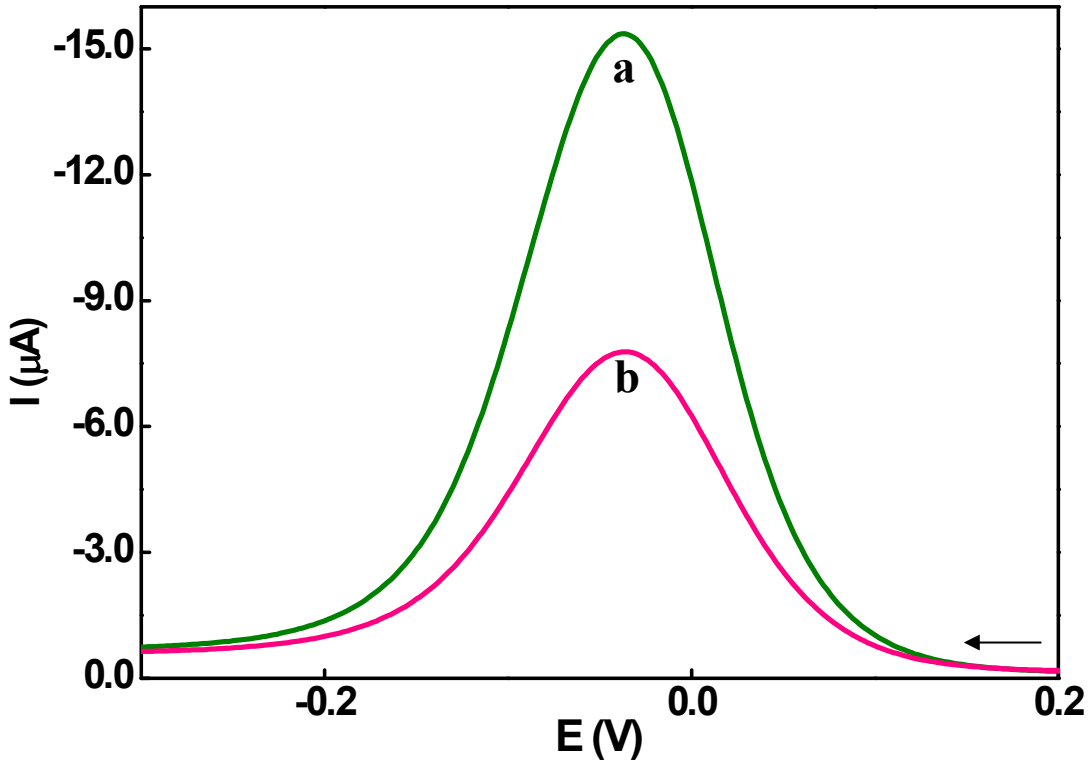

Fig. S20 Differential pulse voltammograms of **1** (0.5 mM) in the absence (a) and presence (b) of CT DNA (R = 5) at 25.0 ± 0.2 °C at 2 mV s^{-1} scan rate in 2% DMF/5mM Tris-HCl/50 mM NaCl buffer at pH 7.1.

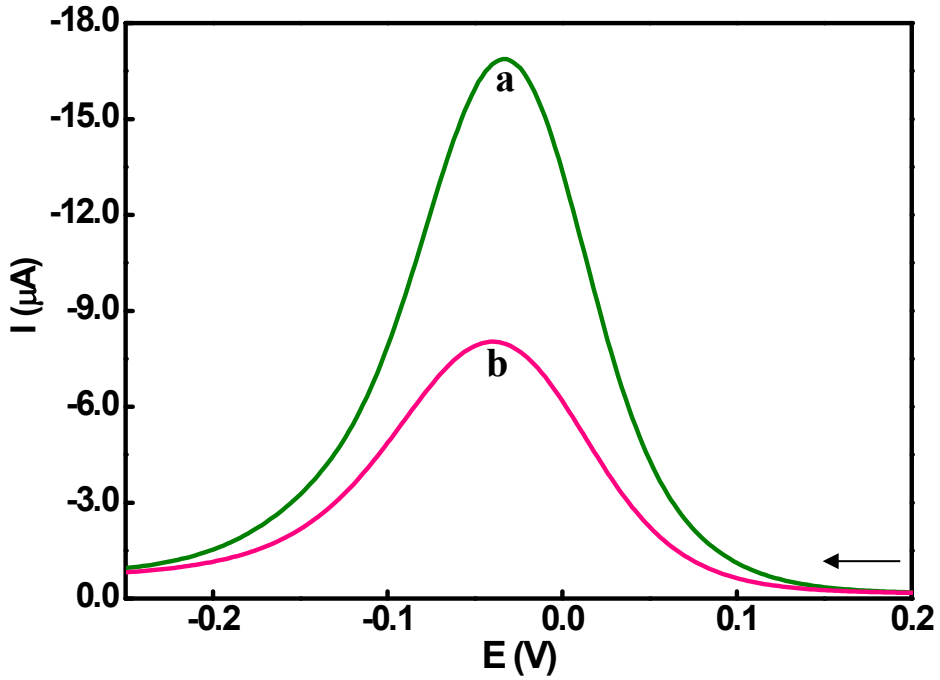

Fig. S21 Differential pulse voltammograms of **2** (0.5 mM) in the absence (a) and presence (b) of CT DNA (R = 5) at 25.0 ± 0.2 °C at 2 mV s^{-1} scan rate in 2% DMF/5mM Tris-HCl/50 mM NaCl buffer at pH 7.1.

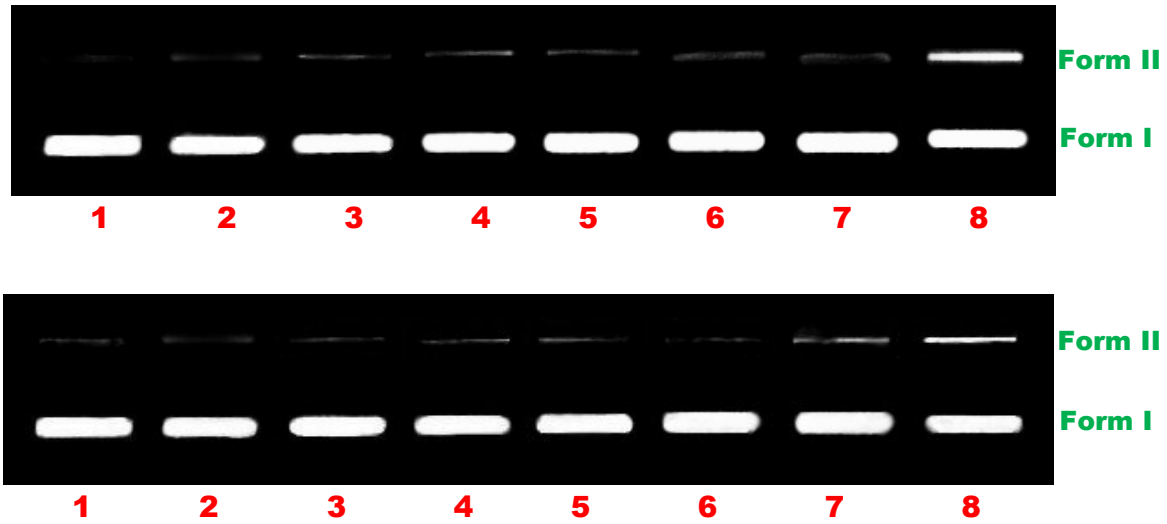

Fig. S22 Agarose gel showing cleavage of 20 μM SC pUC19 DNA incubated with **1** (top) or **2** (bottom) in 2% DMF 50 mM Tris-HCl/NaCl buffer (pH 7.1) at 37 °C for 1 h. Lane 1, DNA; lanes 2-8, DNA + **1** (top) or **2** (bottom) (10, 20, 30, 40, 60, 80, 100 μM respectively). Forms I and II are supercoiled and nicked circular forms of DNA respectively.

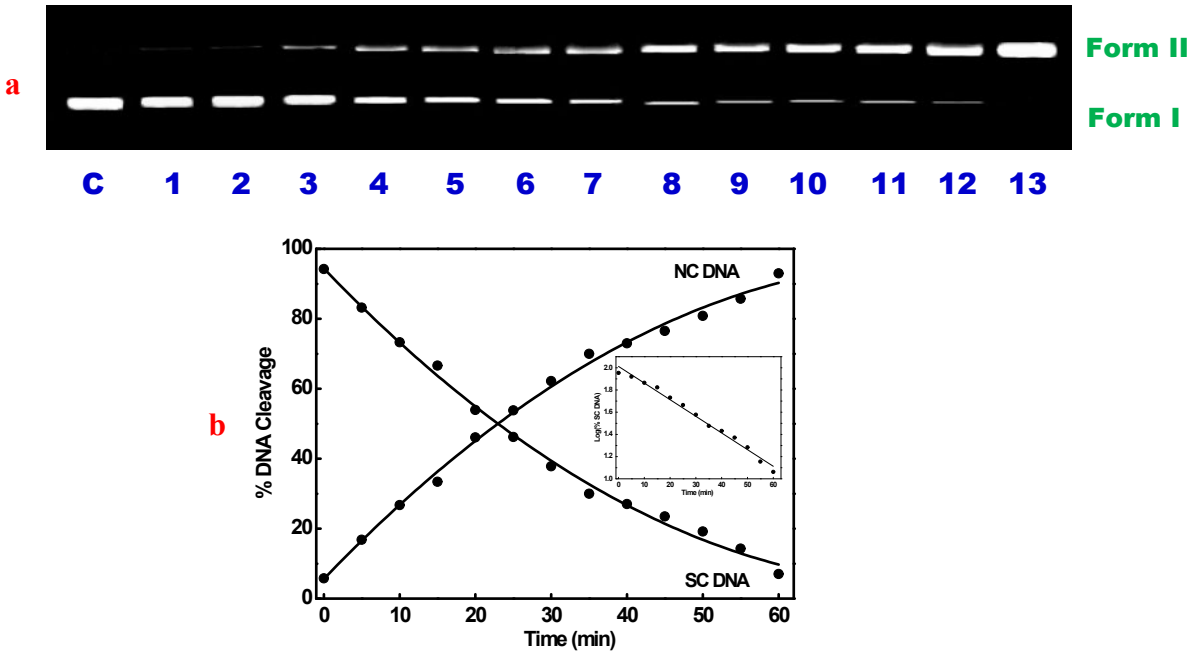

Fig. S23 (a) Agarose gel showing cleavage of 140 μM SC pUC19 DNA incubated with **2** (130 μM) in 2% DMF 50mM Tris-HCl/NaCl buffer (pH 7.1) at 37 °C for 1 h. Lane C, DNA; lanes 1-13, DNA + **2** (0, 5, 10, 15, 20, 25, 30, 35, 40, 45, 50, 55, 60 h respectively). Forms I and II are supercoiled and nicked circular forms of DNA respectively and (b) disappearance of the supercoiled form (SC DNA) and formation of the nicked circular form. Inset: (% SC DNA) versus time for a **2** (130 μM).

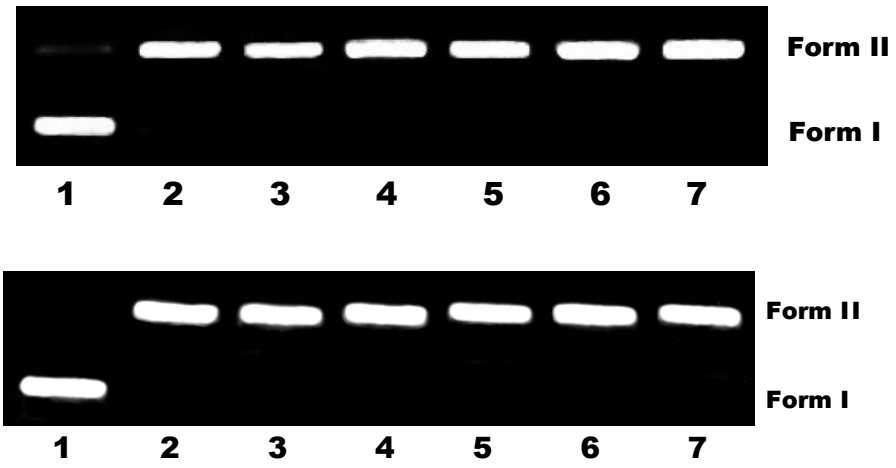

Fig. S24 Agarose gel showing cleavage of 20 μM SC pUC19 DNA incubated with 30 μM **1** (top) or **2** (bottom) in 2% DMF 50mM Tris-HCl/NaCl buffer (pH 7.1) at 37 °C for 1 h. Lane 1, DNA; Lane 2, : DNA + **1** (top) or **2** (bottom), Lane 3: DNA + **1** (top) or **2** (bottom) + NaN_3 (100 μM), Lane 4: DNA + **1** (top) or **2** (bottom) + Methyl Green (100 μM), Lane 5: DNA + **1** (top) or **2** (bottom) + DMSO (20 μM), Lane 6: DNA + **1** (top) or **2** (bottom) + SOD (0.5 units), Lane 7: DNA + **1** (top) or **2** (bottom) + Catalase (0.5 units).

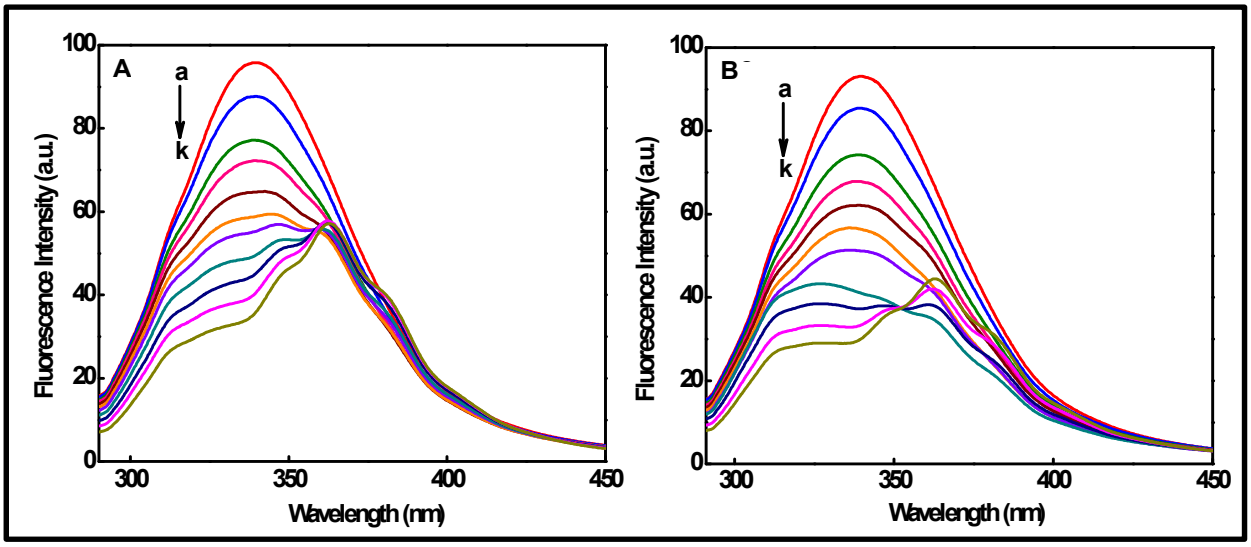

Fig. S25 Changes in the fluorescence spectra of BSA through the titration with **2** at 300 K (left, **A**) and 310 K (right, **B**). The concentration of BSA is 1×10^{-6} mol L^{-1}, and the concentration of **2** was varied from (a) 0.0 to (k) 4.0×10^{-6} mol L^{-1}; pH 7.4 and λ_{ex} 280 nm.

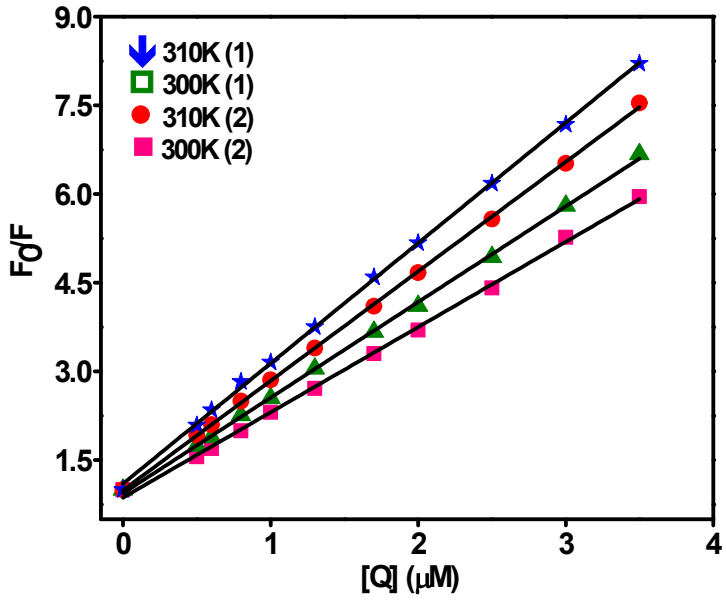

Fig. S26 The Stern-Volmer plots of BSA at different temperatures for addition of **1** and **2**. λ_{ex} = 280 nm; pH = 7.4.

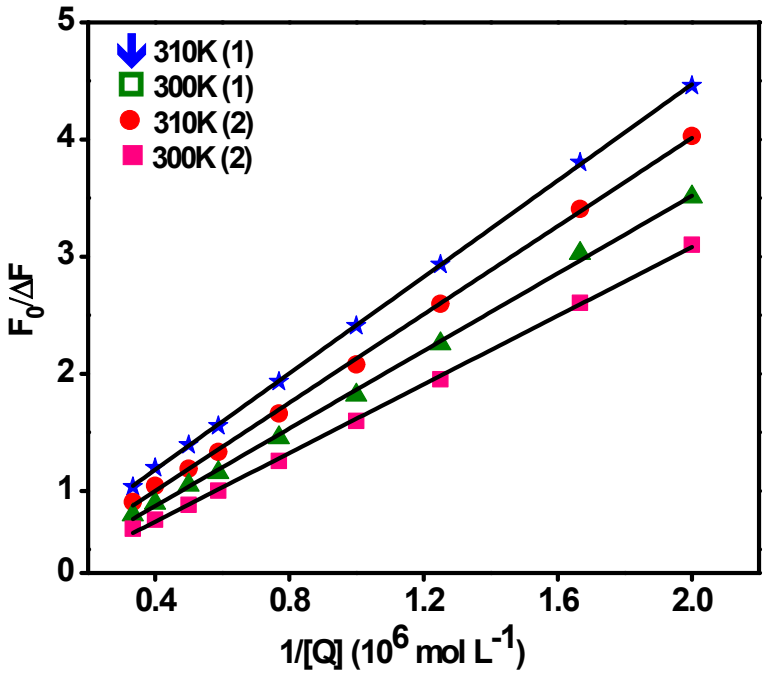

Fig. S27 The modified Stern-Volmer plots of BSA at different temperatures for addition of **1** and **2**. λ_{ex} = 280 nm; pH = 7.4.

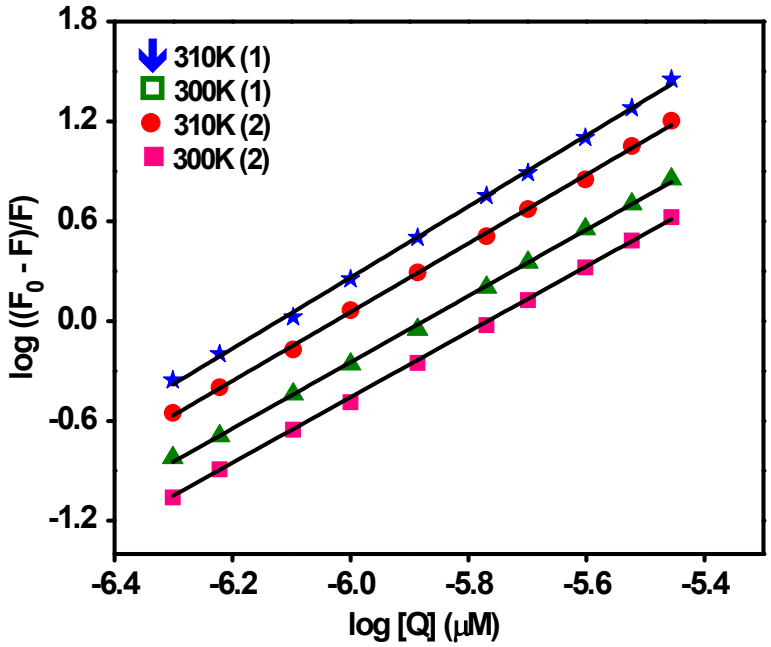

Fig. S28 Double-log plot of quenching effect of **1** and **2** on BSA fluorescence at pH = 7.4.

DNA binding experiments

Concentrated stock solutions of DNA (13.5 mol dm^3) were prepared in buffer and sonicated for 25 cycles, where each cycle consisted of 30 s with 1 min intervals. For absorption and emission spectral experiments, the DNA solutions were pretreated with solutions of copper(II) complexes to ensure no change in concentration of the copper(II) complex.

Absorption spectral titration experiments were performed by maintaining a constant concentration of the complex and varying the nucleic acid concentration. This was achieved by dissolving an appropriate amount of the metal complex and DNA stock solutions while maintaining the total volume constant (1 mL). This results in a series of solutions with varying concentrations of DNA, but with a constant concentration of the complex. The absorbance (A) of the most red-shifted band of the complex was recorded after successive additions of CT DNA.

Circular dichroic (CD) spectral experiments were done using a cylindrical 0.1 cm path length quartz cell. Each CD spectrum was collected after averaging over at least four accumulations using a scan speed of 100 nm min^{-1} and 1 s response time. Machine plus cuvette baselines were subtracted and the resultant spectrum zeroed outside the absorption bands.

For emission intensity measurements, the 2% DMF/50mM Tris-HCl/50 mM NaCl buffer was used as a blank to make preliminary adjustments. The excitation wavelength was fixed and the emission range was adjusted before measurements. DNA was pretreated with ethidium bromide in the ratio [NP]:[EthBr] = 1:1 for 30 min at 27 °C. The metal complex was then added to this mixture and their effect on the emission intensity was measured.

Cyclic voltammetry (CV) and differential pulse voltammetry (DPV) were performed in a CHI 620C electrochemical analyzer at 25 ± 0.2 °C. The working electrode was a glassy carbon disk (0.0707 cm^2) and the reference electrode, a saturated calomel electrode. A platinum wire was used as the counter electrode. The supporting electrolyte was Tris-HCl/50 mM NaCl buffer (pH 7.1). Solutions were deoxygenated by purging with nitrogen gas for 15 min prior to measurements; during measurements a stream of N_2 gas was passed over them. The redox potential $E_{1/2}$ was calculated from the anodic (E_{pa}) and cathodic (E_{pc}) peak potentials of CV traces as $(E_{pa} + E_{pc})/2$ and also from the peak potential (E_p) of DPV response as $E_p + \Delta E/2$ (ΔE is the pulse height).

Protein Binding Experiments

All fluorescence measurements were performed using a 10 mm quartz cuvette at two different temperatures (300 and 310 K). Quantitative analyses of the interaction between complex and BSA were performed by fluorimetric titration (0.05 M phosphate buffer, pH 7.4). A 3.0 mL portion of an aqueous solution of BSA was titrated by successive additions of the complex. Titrations were done manually by using an Eppendorf micro pipette. For every addition, the mixture solution was shaken and allowed to stand for 20 min at the corresponding temperature (300 and 310 K) and then the fluorescence intensities were measured with an excitation wavelength of 280 nm and emission wavelengths in the interval 290-500 nm. The data were corrected using the inner filter effect. The excitation and emission slit width (each 5.0 nm), scan rate (fast) were constantly maintained for all the experiments. The UV-Visible absorption spectra of 1.0 μM free BSA as well as BSA/complex (equal molar ratio) in 0.5 M phosphate buffer of pH 7.4 were recorded from 200-500 nm.

Calculation of BSA Binding Parameters Fluorescence quenching property can be described by the Stern-Volmer equation:[1]

$$F_0/F = 1 + K_{SV}[Q] = 1 + k_q\tau_0[Q]$$

where F_0 and F are the steady-state fluorescence intensities in the absence and the presence of quencher, respectively. K_{SV} is the Stern-Volmer quenching constant and [Q] is the concentration of quencher. The plot of F_0/F *versus* [Q] shows the value of K_{SV}. According to the above equation

$$K_{SV} = k_q/\tau_0$$

where K_q is the quenching rate constant and τ_0 is the fluorescence lifetime of protein in the absence of quencher, the value of τ_0 is considered to be 10^{-8} s.[2]

The binding constant (K_b) and the numbers of binding sites (n) can be determined using the following equation:[3]

$$\log[F_0\text{-}F/F] = \log K_b + n\log[Q]$$

where K_b is the binding constant, reflecting the degree of interaction of the BSA and complex, and n is the number of binding sites. The plots of $\log[(F_0\text{-}F)/F]$ *versus* log[Q] gives a straight line. The values of n and K_b can be calculated from the slope and intercept of the linear plot respectively.

The thermodynamic parameters can be calculated from the following Van't Hoff equations[4,5] to elucidate the binding forces between complex and BSA.

$$\ln(K_2/K_1) = (1/T_1 - 1/T_2)\, \Delta H^\circ/R$$

$$\Delta G^\circ = \Delta H^\circ - T\Delta S^\circ = -RT\ln K$$

where K_1 and K_2 are equilibrium binding constants at temperature T_1 and T_2, respectively, and R is the gas constant.

References

1. J. R. Lakowicz, *Principles of Fluorescence Spectroscopy*, 3rd edn, Springer Science + Business Media, New York, 2006.
2. J. R. Lakowicz and G. Webber, *Biochemistry*, 1973, **12**, 4161–4170.
3. T. Wang, Z. Zhao, B. Wei, L. Zhang and L. Ji, *J. Mol. Struct.*, 2010, **970**, 128–133.
4. J. B. F. Lloyd and I. W. Evett, *Anal. Chem.*, 1977, **49**, 1710–1715.
5. J. Jayabharathi, V. Thanikachalam and M. V. Perumal, *Spectrochim. Acta, Part A*, 2011, **79**, 502-507.